

Star formation intensities of non-isolated galaxies with the CALIFA survey



A. Morales^{1★}, F. F. Rosales-Ortega², J. P. Torres-Papaqui¹, S. F. Sánchez³, M. Chow-Martínez¹, R. A. Ortega-Minakata³, F. J. Romero-Cruz¹, J. J. Trejo-Alonso⁴, D. M. Neri-Larios⁵, A. Robleto-Orús¹ & the CALIFA collaboration⁶

¹Universidad de Guanajuato ²Instituto Nacional de Astrofísica, Óptica y Electrónica ³Instituto de Astronomía, Universidad Nacional Autónoma de México ⁴Facultad de Ingeniería, Universidad Autónoma de Querétaro ⁵The University of Melbourne ⁶<http://califa.caha.es/>

Introduction

Galaxy evolution is turned on by star formation (SF). In order to quantify the latter, star formation rates (SFRs) are computed measuring gas recombination emission lines (indirect consequences of young-massive and strongly-ionizing stars). Galaxy surveys with potential spatial resolution techniques (Integral Field Spectroscopy) such as the CALIFA survey^[1], enable us to resolve typical key regions where SF occurs. The CALIFA survey is then perfectly suitable to trace the structural variation of the SF by means of the **intensity of the SFR (Σ_{SFR})**.

Goals

1. To distinguish between forced and passive SF processes by comparing the Σ_{SFR} annulus structures of galaxies in opposed environmental scenarios.
2. To find out if the Σ_{SFR} might be a function of the degree of galaxy interactions.
3. To confirm the general trend of galactic formation from the inside-out^[2,3].

Current instances

Using the theory of tidal perturbation^[4], *non-isolated* and *isolated* CALIFA galaxies are selected in order to compare their stellar properties. The Σ_{SFR} , the stellar mass (M_*) and the stellar population (SP) age annulus structures are explored. We are determining whether the highest Σ_{SFR} values (per spaxel) are near/around the galaxy centers. These highest values, the cause of the chemical differences among galaxies^[5], might be related to de degree of interactions.

Methods

- ▶ Adjusting SP models to CALIFA survey spectra (STARLIGHT^[6]).
- ▶ Fitting gaussian profiles to the emission line residuals.
- ▶ Imposing an H α EW cut-off ($\geq 6 \text{ \AA}$) characteristic of emission line (H β S/N ≥ 3) and star-forming galaxies ([O II] and [O III] S/N ≥ 3)^[7], and also proper of H II regions with high fractions of young SPs^[8].
- ▶ Selection of reliable SF spaxels by means of diagnostic diagrams (DDs)^[9] and several H II region/Starburst instantaneous and evolving models^[10].
- ▶ Estimating Σ_{SFR} (using the extinction-corrected H α line flux), mean SP age and stellar mass (density) structures by spatial annuli.

Results

1. The left-side of Fig. 1 compares our sample fits with the main sequence of SF (MSSF)^[11]. The non-isolated sample fit differs the most from the yellow line, suggesting the SFRs of these galaxies depending the least on M_* . Moreover, positive and negative mass differences in the isolated sample (center of Fig. 1) cancel out. Both differences, in the non-isolated sample (right), are correlated with M_* , notoriously, for positive values. For these we draw subfits (orange lines depending on whether M_* is lower or greater than $\log_{10} 10 M_{\odot}$). The solid subfit is the steepest so, for influenced galaxies with $\log_{10} 10.8 M_{\odot}$, the mass average of galaxies which differences trace the solid subfit, the SFRs depend less on M_* to do more on interactions. Figure 2 gives support to this assertion.
2. Figure 3 shows each samples' Σ_{SFR} structures by trend, 1: a continuous decrease from the center, and 2: otherwise. The greatest Σ_{SFR} falls in the innermost annulus of the non-isolated sample (C label) with poor SF in the next annuli. The isolated sample shows clear presence of SF all along the annuli (D label). C supports interactions as facilitators of the angular momentum lost conveying most of gas to the center whereas D exemplifies passive, steady long-lived evolution. A decreasing sequence regarding the strength of the active galactic nucleus (AGN) activity: A, B, C and D (by using DDs^[9]) is found.

References

- [1] S. F. Sánchez, R. C. Kennicutt, A. Gil de Paz, and *et al.* *A&A*, 538:31, 2012.
- [2] R. M. González Delgado, R. García-Benito, E. Pérez, and *et al.* *A&A*, 581:44, 2015.
- [3] Z. Zheng, H. Wang, J. Ge, and *et al.* *MNRAS*, 465:16, 2017.
- [4] J. Varela, M. Moles, I. Márquez, and *et al.* *A&A*, 420:873–879, 2004.
- [5] J. P. Torres-Papaqui, R. Coziol, R. A. Ortega-Minakata, and *et al.* *ApJ*, 754:24, 2012.
- [6] R. Cid Fernandes, A. Mateus, L. Sodré, and *et al.* *MNRAS*, 358:363–378, 2005.
- [7] R. Cid Fernandes, G. Stasińska, M. S. Schlickmann, and *et al.* *MNRAS*, 403:17, 2010.
- [8] S. F. Sánchez, F. F. Rosales-Ortega, J. Iglesias-Páramo, and *et al.* *A&A*, 563:25, 2014.
- [9] J. A. Baldwin, M. M. Phillips, and R. Terlevich. *PASP*, 93:5, 1981.
- [10] L. J. Kewley, M. A. Dopita, R. S. Sutherland, and *et al.* *ApJ*, 556:19, 2001.
- [11] A. Renzini and Y.-j. Peng. *ApJ*, 801:6, 2015.

Figures

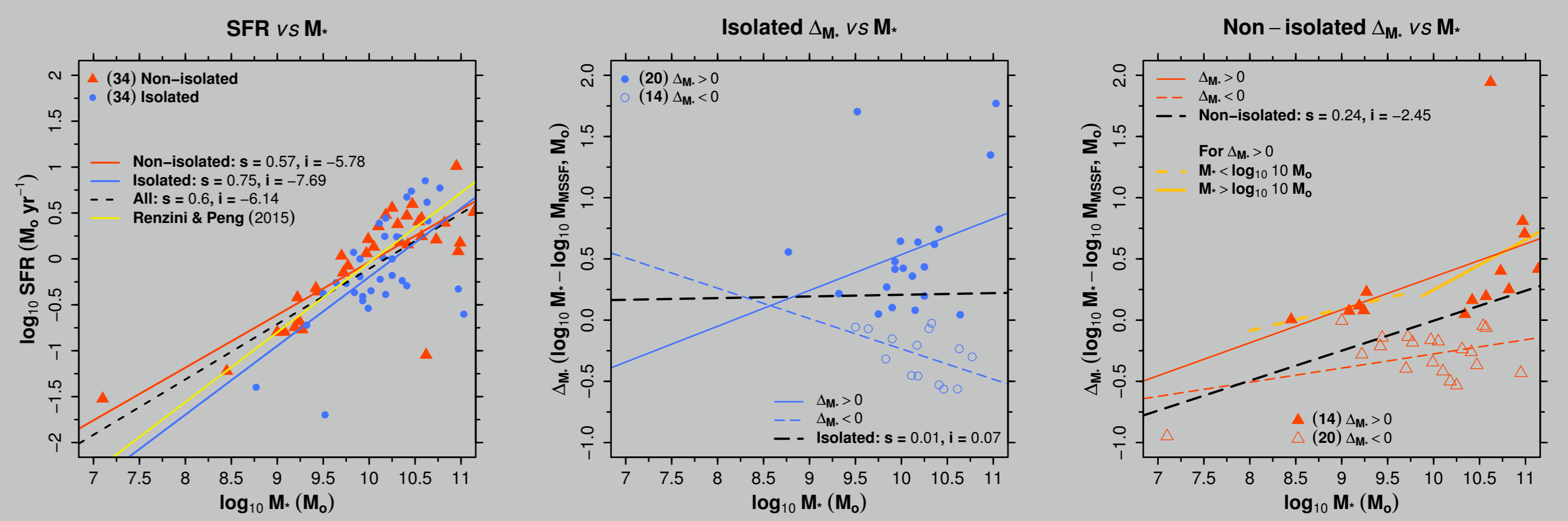


Figure 1: Linear fits (left) in the SFR vs global M_* plane (red: non-isolated, blue: isolated, dashed line: both samples). The MSSF^[11] ($s = 0.76$, $i = -7.64$) is represented by the yellow line. ΔM_* ($\log_{10} M_* - \log_{10} M_{MSSF}$) vs M_* for isolated (center) and non-isolated (right) galaxies. M_{MSSF} indicates the resulting stellar masses if our galaxies would obey the fit by^[11] (see the left panel). Filled and empty symbols respectively represent positive and negative ΔM_* values while the blue and red lines their respective fits (solid: $\Delta M_* > 0$, dashed: $\Delta M_* < 0$). Black dashed lines are the fits of all symbols. Subfits for positive ΔM_* values, in the non-isolated sample, are indicated by the orange lines (dashed: $M_* < \log_{10} 10 M_{\odot}$, solid: $M_* > \log_{10} 10 M_{\odot}$). With these subfits we propose a critical mass, $M_{crit} \geq 6.40 \times 10^{10} M_{\odot}$ ($\log_{10} 10.8 M_{\odot}$, see text), as a lower limit from which the SFR depends more on the interactions than on stellar mass.

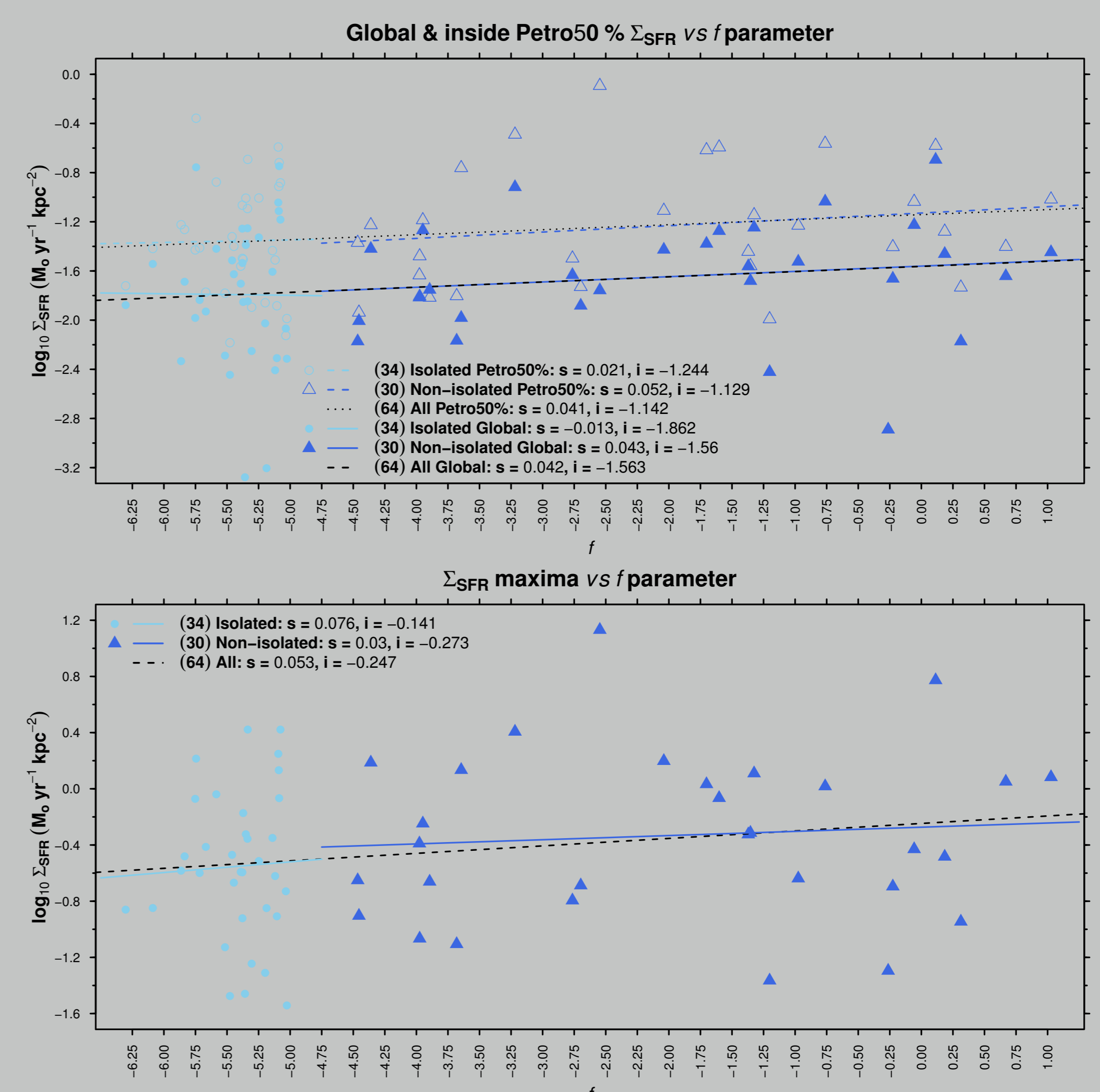


Figure 2: The Σ_{SFR} vs the tidal influence parameter f ^[4]: (top) global and inside the Petro50% radius (which encloses 50% of the flux in the r band) and (bottom) each galaxy's maximum (maximum spaxel). An increment of the Σ_{SFR} with f is observed. The slopes (s) of the estimated fits, independently of their low values (irrelevant fact since the contrast between scales), are all positive except one. Larger slopes belong to the isolated sample due to its narrower f range of values.

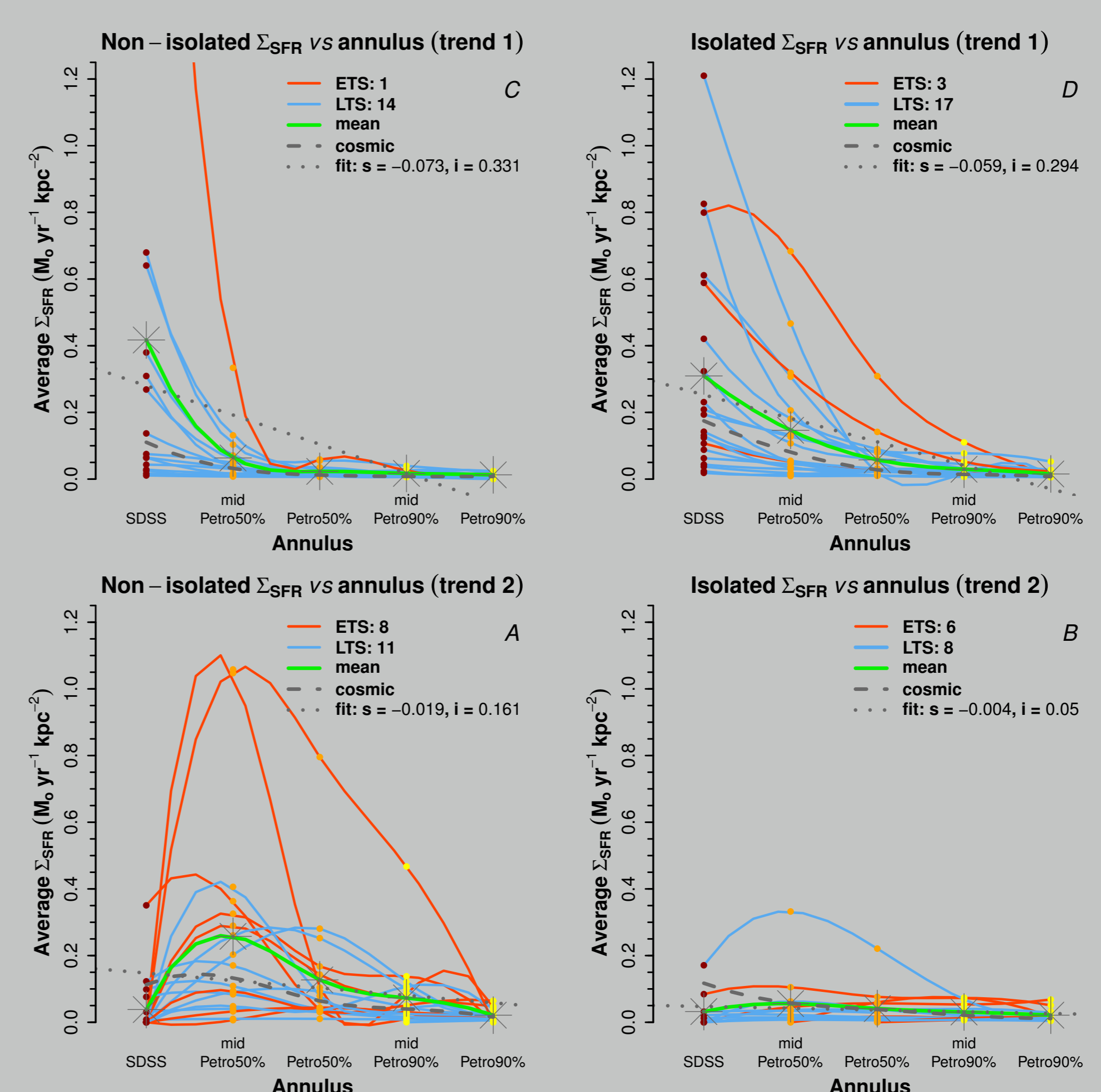


Figure 3: The Σ_{SFR} structures (all gradients being negative support the inside-out formation of the SPs^[2,3]). Trends and morphological groups: ETSs (early type spirals) and LTS (late type spirals). The radial distance is represented by five consecutive-outward annuli: "SDSS", "midPetro50%", "Petro50%", "midPetro90%" and "Petro90%". Each vertically-aligned color point (brown, orange and yellow), indicates each galaxy's spaxel average in such respective annulus. The $\Sigma_{SFR}^{SDSS} \sim 3.520 M_{\odot} \text{ yr}^{-1} \text{ kpc}^{-2}$ of NGC5930 in the top left, overpasses the scale range of the left. Green lines (mean) connect the average (asterisks) of the color points by annulus. Dashed lines (cosmic) show the Σ_{SFR} assuming a constant SFR during the Hubble time. Dotted lines (fit) indicate linear fits of all points. Alphabetical labels in reference to text.